

OPTIMIZATION OF VOLUMETRIC EFFICIENCY OF A SMALL WANKEL ENGINE USING GENETIC ALGORITHM

by

Yan ZHANG , Jinxiang LIU* , Zhengxing ZUO, and Shuai ZHANG

School of Mechanical Engineering, Beijing Institute of Technology, Beijing, China

Original scientific paper
<https://doi.org/10.2298/TSCI180504058Z>

In this work, port crank angles strategies for maximizing engine volumetric efficiency of a commercial rotary engine are studied. The internal combustion engines computer program, which simulates an actual working processes, has been used. Overall performance characteristics such as the cycle efficiency, engine power are calculated by a mathematical model. The model is calibrated with data obtain from a measured in-cylinder pressure, and validated against the experimental data. Intake opening and closing time, exhaust opening and closing time are chosen as optimization variables when volumetric efficiency was taken as the objective function. First, the intake opening time is the only optimization variable and it can be found that intake opening time is in advance as engine speed is increased. Second, four variables including intake opening and closing, exhaust opening and closing have been taken as the optimization variables, a further increase in volumetric efficiency was obtained, with the highest gain being of 1.03% at 17000 rpm. But opening the exhaust opening very late will reduce the power.

Key words: *volumetric efficiency, Wankel engine, genetic algorithm*

Introduction

The small Wankel engine provides higher power density, lower vibration, and fewer parts than conventional piston engines [1]. It can be used in recreational vehicles, portable devices as well as other small equipments where the smaller volume and the lighter weight are needed [2]. However, the problem that the thermal efficiency is very low in small Wankel engine has not been solved yet. Based on this problem, some investigations on the conventional piston engines have indicated that suitable intake and exhaust crank angle (CA) can improve this problem considerably [3, 4]. Different from variable valve timing in conventional piston engines, the intake and exhaust port CA of rotary engines are fixed. Therefore, the study on port CA of small Wankel engine is very necessary.

A wide study about the effects of valve timing on conventional engines performances have been carried out [5-7]. However, there are few researches about the effect of port CA on small Wankel engines. Due to the similar thermodynamic processes between the small Wankel engine and the conventional piston engines, this paper can take previous method to optimize the port CA. Different optimization techniques have been employed in the study of internal combustion engines. D'Errico *et al.* [8] chose the mesh adaptive direct search (MADS) method among the class of direct search methods and compared with the genetic algorithms (GA) to solve single-objective problems and multi-objective problems. The MADS

* Corresponding author, e-mail: liujx@bit.edu.cn

as an exact optimization methodology usually spend more time on iterations and searching. Sher *et al.* [9] postulate optimal valve strategies for minimizing fuel consumption or maximizing engine torque in term of the intake and exhaust valve phases of gasoline using variable valve timing technology. The calculation accuracy of this method is not enough high. Zhao *et al.* [10] combined 1-D software GT-POWER with a genetic code optimize the processes of the gas change for the Atkinson cycle engine. The GA is less likely to get trapped in local minima and is not restricted by continuity. Och *et al.* [11] chosen duct lengths and valve timing as optimization variables to optimize the volumetric efficiency of a single-cylinder diesel engine based on the differential evolution technique. Therefore, the GA is chosen as the optimization technique in our work.

It is the purpose of the present paper to optimize port CA in order to maximizing volumetric efficiency using GA. In this work, first, a 1-D mathematical model of gas exchanges and in-cylinder processes is established. Second, this model is validated and calibrated by experimental data. Third, using GA maximizes volumetric efficiency by optimizing port CA.

Engine model

Working principle of Wankel engine

The working processes of Wankel engine include intake, compression, combustion and expansion, exhaust shown in fig. 1. The position that the volume of the chamber is smallest is as TDC. This paper takes OS-49 as the object to realize the optimization. The specifications of this engine are given in tab. 1.

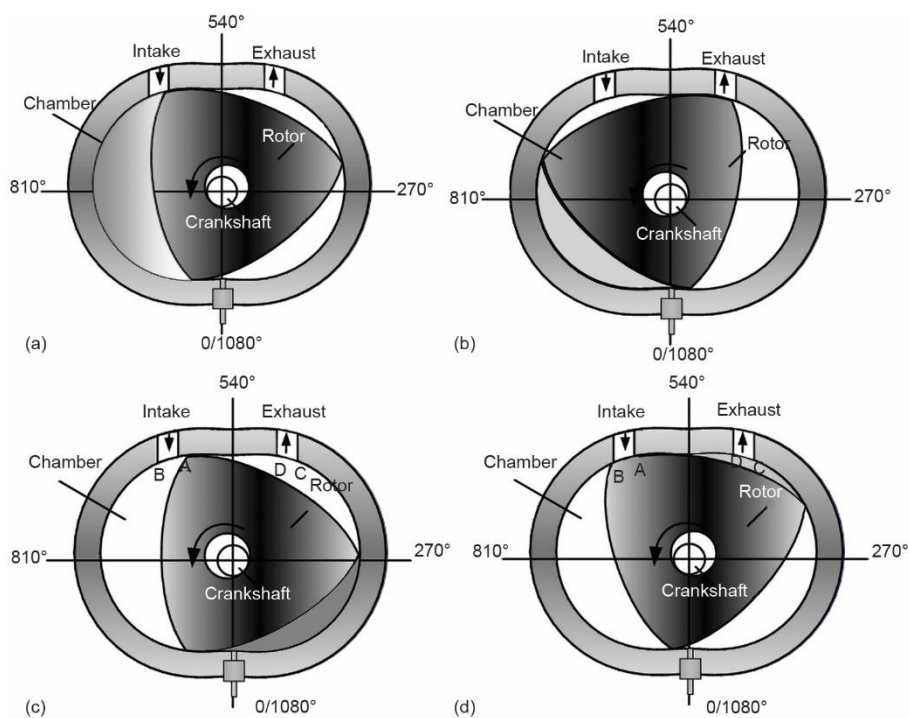


Figure 1. Working principle of the Wankel engine; (a) intake, (b) compression, (c) combustion and expansion, (d) exhaust

Table 1. Engine specification

Engine model	O.S. 49-II
Engine type	Wankel engine
Displacement volume	4950 mm ³
Number of rotors	1
Intake and exhaust mode	Peripheral intake and exhaust
Intake phase	460° (80° bTDC), 885° (75° aBDC)
Exhaust phase	188° (82° bBDC), 578° (38° aBDC)

Mathematical model

Cylinder content

The analysis is based on a set of 1-D conservation equations written [12]:

$$\dot{Q} = \dot{W} + \frac{dE}{dt} + \sum \dot{m}_e h_e - \sum \dot{m}_i h_i \quad (1)$$

$$p \frac{dV}{dt} + V \frac{dp}{dt} = m_c R \frac{dT}{dt} + RgT \frac{dm_c}{dt} \quad (2)$$

where \dot{W} is the rate of work done by the open system, $\dot{Q} = \dot{Q}_c + \dot{Q}_w$, \dot{Q}_c – the rate of heat releases during combustion, \dot{Q}_w – the rate of heat transfer from the cylinder wall, front, and backcovers, rotor to the cylinder contents, dE/dt – the rate of energy increase inside the open system, which is equal to $d(m_c v T)/dt$, h_e and h_i – the enthalpies of the leaving and entering enthalpy through the ports, respectively, and Rg – the gas constant. The mass conservation equation can be written:

$$\frac{dm_c}{dt} = \frac{dm_{in}}{dt} - \frac{dm_e}{dt} \quad (3)$$

Equations (1) and (2) by introducing mass conservation eq. (3) can be written:

$$\frac{dp}{dt} = \frac{\gamma - 1}{V} \left(\frac{dQ_c}{dt} + \frac{dQ_w}{dt} \right) - \gamma p \frac{dV}{dt} + (\gamma - 1) \left(\sum_i \dot{m}_i c_p T_i - \sum_e \dot{m}_e c_p T_e \right) \quad (4)$$

where γ is the instantaneous specific heat ratio.

The V represents the volume of the chamber depicted by eq. (5).

$$V = \left[\frac{\pi}{3} + 2\sqrt{K^2 - 9} - \frac{3\sqrt{3}}{2} K \sin\left(\frac{2}{3}\theta + \frac{\pi}{6}\right) + \left(\frac{2}{9}K^2 + 4\right) \phi_{\max} \right] e^2 B \quad (5)$$

where R is rotor radius, e is eccentricity of the output shaft, $K = R/e$, $\phi_{\max} = \arcsin[3e/(R + a)]$, a is translational distance, and B is the width of the rotor.

For small rotary engine, the intake port is directly connected with the carburetor. The inlet of carburetor is communicated with the atmosphere. So the intake mass is decided by the pressure difference and the throttle opening. The instantaneous mass flow rate, \dot{m} is determined by:

$$\dot{m} = A \left(\frac{2\gamma p_H \rho_H g}{\gamma - 1} \right)^{1/2} y^{1/\gamma} \left(1 - y^{\frac{\gamma-1}{\gamma}} \right)^{1/2} \quad (6)$$

where $y = p_L/p_H$, A is the instantaneous effective port area, which was taken as 80% for its actual value, and H and L denote upstream and downstream conditions, respectively.

The combustion process is taken as one step global reaction scheme. The mass fraction burned at any angle is written as [13, 14]:

$$X = 1 - \exp \left[-6.908 \left(\frac{\theta - \theta_0}{\theta_z} \right)^{a+1} \right] \quad (7)$$

The combustion velocity of the mixture in cylinder is calculated by Wiebe function [14]:

$$\frac{dX}{d\theta} = 6.908 \frac{a+1}{\theta_z} \left(\frac{\theta - \theta_0}{\theta_z} \right) \exp \left[-6.908 \left(\frac{\theta - \theta_0}{\theta_z} \right)^{a+1} \right] \quad (8)$$

where a is the combustion quality index, θ_z – the crank angle corresponding to the sustained combustion period, θ_0 – the crank angle at the beginning of the combustion.

Then, the heat release rate of fuel related to the combustion velocity can be written [15]:

$$\frac{dQ_c}{d\theta} = H_u m_f \frac{dX}{d\theta} \quad (9)$$

where H_u , and m_f represent fuel calorific value and fuel feed. For the small rotary engine, the mixture of air and vaporized fuel is delivered to the cylinder by the carburetor. Energy losses for Wankel engine are considerable through the rotor, the side covers and the cylinder. Since the Wankel engine have characteristically large surface to volume ratios and velocity gradients at stationary surface, the heat transfer rate is relative high.

The heat loss can be calculated by [16, 17]:

$$\frac{dQ_w}{dt} = h_g \left[A_{rot}(T - T_{rot}) + A_{cyl}(T - T_{cyl}) + A_{cov}(T - T_{cov}) \right] \quad (10)$$

Using Woshni's for thermal conductivity, the heat transfer coefficient yields:

$$h_g = 110d^{-2}P^{0.8}T^{-0.53}W^{0.8} \quad (11)$$

where d is characteristic length of rotary engine, $d = 2(1/B + BL/V)$, W is gas velocity.

Optimization techniques

The GA is an efficient tool for solving the multi-object complex problems. The GA mimics the natural evolutionary process by introducing the principles of survival of fittest and genetic theory. The method is divided into three steps: mutation, crossover, and selection.

In a multiobjective optimization problem different objectives must be optimized simultaneously, with regard to some constraints. Mathematically, the problem can be written as follows:

$$F(x) = \begin{bmatrix} f_1(x) \\ f_2(x) \\ \vdots \\ f_n(x) \end{bmatrix} \quad (12)$$

with

$$\begin{cases} h_i(x) = 0 \\ g_i(x) \leq 0 \\ x_{k,\min} \leq x_k \leq x_{k,\max} \end{cases}$$

In this equation, x represents the set of variables to be optimized, $F(x)$ is the vector of objectives, $h_i(x)$ and $g_i(x)$ are the equality and inequality constraints, and $x_{k,\min}$ is the range to which the variables belong.

In this paper, volumetric efficiency as the objective function is order to optimize the port CA. A mathematical model [9], is employed to simulate the gas change process inside the cylinder during the valve overlap period. The instantaneous volumetric efficiency is calculated by:

$$\eta_{ch} = \Lambda - \int_0^\tau \frac{\beta \frac{d\Lambda}{d\tau}}{\beta + (1 + \beta) \frac{T_b}{T_a}} d\tau \quad (13)$$

where T_b and T_a are the temperature of the burned gas and the fresh charge, respectively, Λ – the delivery ratio, τ – the dimensionless crank-angle which is defined by:

$$\tau = \frac{\theta - \theta_{10}}{\theta_{ec} - \theta_{10}} \quad \beta = \frac{\frac{dm_{in}}{dt}}{\frac{dm_e}{dt}} \quad (14)$$

Model validation and calibration

The schematic test bench of the small rotary engine shown in fig. 2. A commercial OS 49 engine mounted on the test bench connects with the torque sensor by a diaphragm coupling MIC-5-0156, which is used to protect the engine and reduce the torque loss. Because the torque of the small rotary engine is very small, a high precision torque master Magtrol 304/111 is selected. Its measurement range is up to 0.6 Nm. The peripheral ported engine with the small combustion chamber depth is tested with methanol as fuel. Methanol and air is mixed upstream of the engine in a carburetor.

Engine speed is measured using a Freescale encoder with a resolution of one °CA degree. The engine is rigidly coupled to the Magtrol dynamometer Dsp 7000 *via* a steel shaft. The engine power and torque is determined by measuring the electrical power generated from the dynamometer. The dynamometer is coupled to the controlled generator CAK CH075016/R by a diaphragm spring type clutch Model ME1052AA. The speed of the controlled generator is up to 50000 rpm. The speed is adjusted by a speed regulator ATVB-2SR 759H.

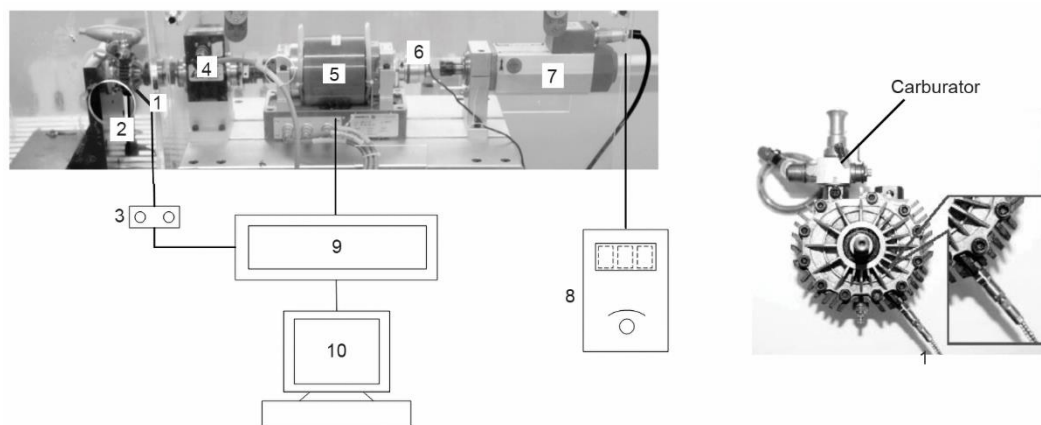


Figure 2. The schematic experimental bench; 1 – pressure transducer, 2 – glow plug, 3 – charge amplifier, 4 – torque sensor, 5 – dynamometer, 6 – clutch, 7 – generator, 8 – machine controller, 9 – data acquisition system, 10 – data record system

The Kistler pressure transducer 6052CU20 is adopted and mounted at the position where expansion process occurs. The transducer signal is amplified by a Kistler charge amplifier 996A27 which is integrated with the CA3004A8 engine combustion analysis instrument. The instrument also acquires and analyses the other signal including the speed, torque, power. The friction power is tested under motoring condition.

Figures 3 and 4 show the comparison of predicted and measured engine brake power, predicted and measured maximum pressure, respectively. The difference of predicted and measured engine brake power is less than 10%, which suggests the predicted method is feasible. The maximum pressure has high randomness so that the difference of predicted and measured maximum pressure is large.

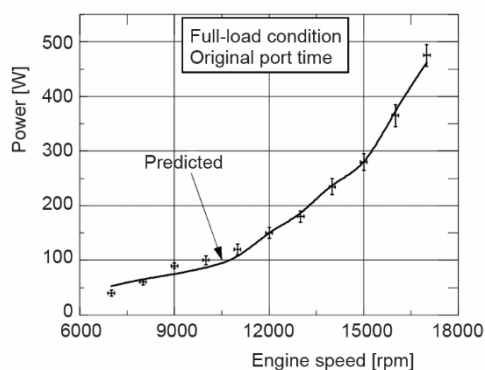


Figure 3. The comparison between the predicted and measured engine brake power for fixed port CA

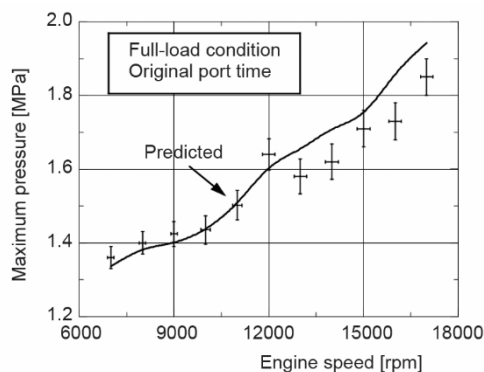


Figure 4. The comparison between the predicted and measured engine maximum pressure for fixed port CA

In order to further validate the predicted model and analyse the working process, pressure in cylinder is compared between the measured and predicted model under the same working conditions. The working speed is at 11000 rpm and the throttle opening is 100%. Figure 5 presents the comparison between the predicted and measured cylinder pressure from compres-

sion to expansion process. The measured data is not for the whole cycle, since the position of the pressure transducer mounted can not acquire the full pressure data, and several pressure transducers can result in leakage for small Wankel engine which is important to engine performance. Therefore, one pressure transducer is adopted to mount on the engine, fig. 2. The maximum difference occurs at the combustion and expansion stage. The reason is that the mixture is ignited by glow plug so that cylinder pressure is not stable. The maximum pressure predicted is higher 7% than the one measured at 11000 rpm since the predicted model does not consider the leakage in the whole working cycle. The methanol calorific value is half the gasoline or diesel, so the cylinder pressure is low relative to other small engine with the same displacement.

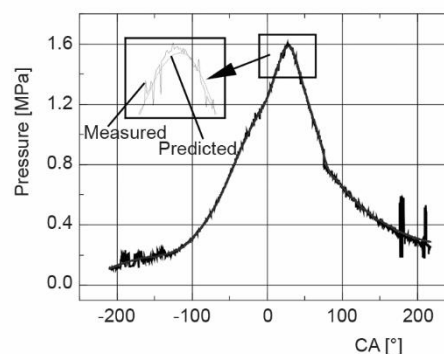


Figure 5. The comparison between the predicted and measured engine cylinder pressure at 11000 rpm

Results and discussions

Table 2 shows the comparison of three methods for volumetric efficiency optimization in small rotary engine. It can be found that the GA presents a better convergence speed than other methods. Besides, the classification accuracy rate of GA is also better. Therefore, GA is selected to compute further.

Table 2. Comparison of three methods

Method	Evolutional generation number	CPU time	Classification accuracy rate
Ant algorithm	600	96 h	94.241
Neural method	400	56 h	93.182
GA	300	48 h	96.254

Once the computational program was validated, the next step is to analyze the small Wankel engine. The port CA of commercial OS-49 engine is taken as a reference for comparison with optimal values obtained later. The intake open angle (IO), intake closed angle (IC), exhaust open angle (EO), and exhaust closed angle (EC) are chosen as optimization variables when volumetric efficiency was taken as the objective function. First, the diameter of intake port keeps unchanged, so the duration time of intake is constant. But the position of intake port changes and the position can be represented by intake opening phase. The intake opening time is the only optimization variable. Second, IO, IC, EO, and EC have been taken as the optimization variables to optimize the volumetric efficiency further.

Figure 6 shows the calculated time area of the intake, which is only relative to position and geometry of the intake port. The time area of Wankel engine yields fixed curve law for different operating conditions. The intake port keeps wide open from 460 CA to 870 CA, which is a long time compared with traditional engine.

Mass-flow rate through the intake port is presented in fig. 7 for different rotary speed. It can be noticed that some outflow precedes the inflow of gas into the cylinder from the beginning of the intake process. For the intake port coming to close, mass-flow shows

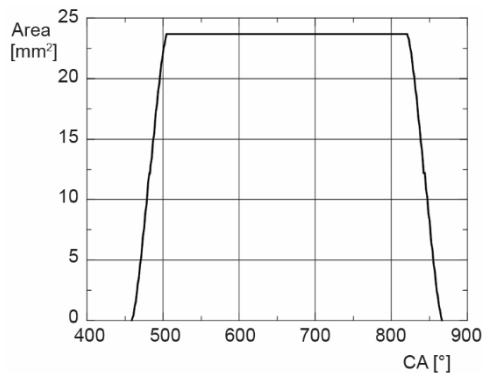


Figure 6. Time area of Wankel engine for intake port

smaller in the lower speed case. The mass outflow at the end of the intake process is higher than the one at the beginning.

In order to compare the optimized results of single and multiple variables based on GA method, the paper discusses the effect of intake CA on the volumetric first. Figure 8 shows the calculated volumetric efficiency as the function of intake port open time for several engine speeds. It is obvious that volumetric efficiency presents maxima and minima with CA. Additionally, it can be observed in fig. 8 that the variation of the volumetric efficiency, resulting from changes from in intake phase, presents a trend of first increase and then decrease. In terms of accuracy and computation cost, the volumetric efficiency values for the referred CA are 0.7722, 0.7870, 0.8192, and 0.8456 for the follow engine speeds: 11000 rpm, 13000 rpm, 15000 rpm, 17000 rpm, respectively. The maximum volumetric efficiency position moves left along the abscissa. Besides, it can be found that the variation range of the volumetric efficiency, resulting from changes in intake port open time, becomes wider when the engine speed increases, and the CA that maximizes volumetric efficiency becomes more narrow as engine speed increases.

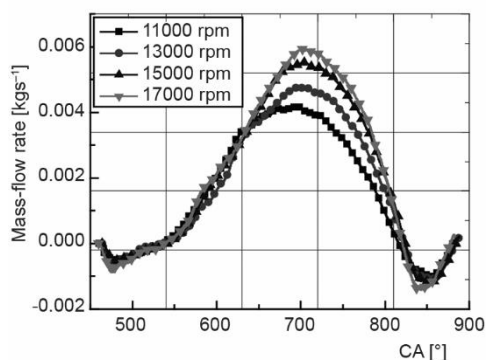


Figure 7. Mass-flow rate as a function of CA

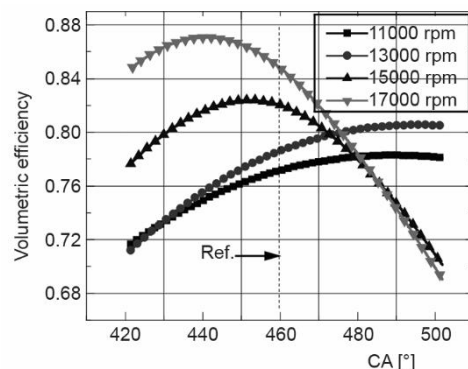


Figure 8. Volumetric efficiency as the function of intake port open time

The intake port diameter keeps constant in fig. 8 and optimization calculation using only one design variable – intake open time. Considering the values in fig. 8 as well as intermediate values of volumetric efficiency calculated using the optimization procedure, fig. 8, it

backflow characteristics. The higher speed case exhibits greater mean mass-flow rate than the lower case in most of the intake process, and reduction of backflow in the intake port, resulting thus, in a higher volumetric efficiency for engine. The maximum at 11000 rpm is 0.00405 kg/s and the one at 17000 rpm is 0.006 kg/s. The maximum difference between the mass-flow rate at 17000 rpm and the value at 11000 rpm is 20%. The difference first increases then decreases with the increase of the rotary speed. It is worth mentioning that at the end of the intake process, mass outflow through the intake port occurs, however, it is

is worth noticing that the optimal volumetric efficiency rises up to the maximum value more quickly as the engine speed increases.

For the small rotary engine, the position of intake port is fixed. The change of intake phase must lead to the variation of the intake port size. In order to keep the intake port diameter unchange and make optimization for the only value of intake open CA, the intake close CA changes with the increase or decrease of intake open CA. Gas mass-flow rate through intake port is shown in fig. 9 for 11000 rpm and 17000 rpm in the case of optimization of the intake port open CA. For the optimization calculation, the intake open CA is used as an optimization variable and by changing this parameter, the volumetric efficiency reaches a maximum for the baseline as well as for the optimized case, which corresponds to intake of quite different open CA (440° and 490°, respectively). It can be clearly noticed in fig. 9 that more outflow for the referred case precedes the inflow of gas into the cylinder from the beginning of the intake process. However, the mass-flow entering the cylinder in the case of the optimization exhibits less flow loss. At the end of the intake process, the optimized and the referred case yields backflow, while the former flow rate is smaller. Therefore, the optimized case shows higher mean mass-flow rate than the referred case in most intake process, and the inhibition of backflow in the intake port, thus, resulting in a higher volumetric efficiency. The increase in volumetric efficiency between the optimized and the referred was 1.5% at 11000 rpm and 3.5% at 17000 rpm. According to the previous investigation [18], the gas velocity through the intake port is high so that gas-flow rate waves propagate from the beginning of the intake. At the beginning and the end of intake process, the waves frequency is low and the amplitude is great. By the optimization calculation, the waves frequency is reduced and backflow in the intake process spends less time. Therefore, the optimal volumetric efficiency is higher than the value for the baseline case.

In fig. 10, it was observed that at 11000 rpm, when exhaust open occurred very late, a low volumetric efficiency and thermal efficiency were obtained. It is attributable to a large amount of pumping work. In contrast, optimal EO occurs before 200 CA, thus without a penalty on engine thermal efficiency and getting a relatively high volumetric efficiency. Base on such a result, optimization calculations were conducted optimizing other variables that EO must occur before 200 CA.

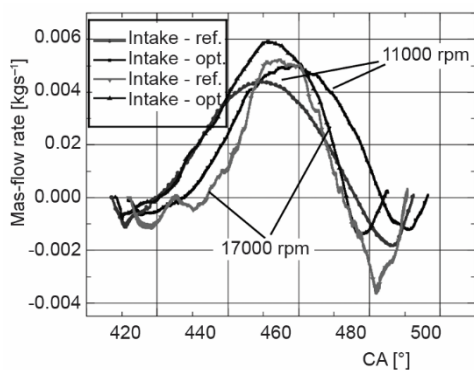


Figure 9. Mass-flow rate as a function of the CA

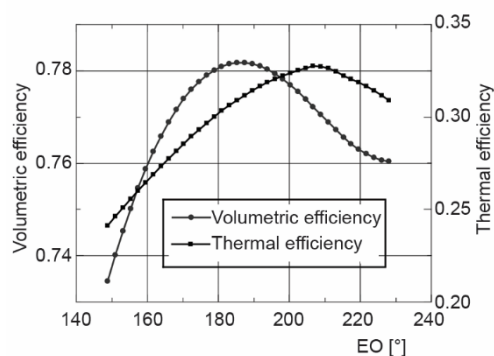


Figure 10. Volumetric efficiency and thermal efficiency as a function of exhaust open angle at 11000 rpm

Table 3 shows the optimized results when four design variables were considered – IO, IC, EO, and EC. Value range for variables changes within plus or minus 40°. Comparing

Table 3. Optimal port time

Speed [rpm]	IO [° bTDC]	IC [° aTDC]	EO [° bTDC]	EC [° aTDC]	Volumetric efficiency	Pe [W]
	80±40	75±40	82±40	83±40		
11000	49.7	39.6	86.6	87.2	0.7918	104.3
13000	59.8	45.1	90.6	89.7	0.8230	189.1
15000	88.6	89	93.1	96.8	0.8632	280.0
17000	100.3	96.5	94.5	102.9	0.8988	470.0

the values shown in those in fig. 8, it can be found that a further increase in volumetric efficiency was obtained, with the highest gain being of 1.03% at 17000 rpm. The results allows us to conclude that the the angle fluctuation of intake open at TDC is larger than the one of intake close at BDC, when the volumetric efficiency is optimized at constant rotary speed. The volumetric efficiency increases with the rising of the engine speed. Results in tab. 3 also indicate that in order to obtain maximum volumetric efficiency, EO and EC must happen, later than they did in the baseline, which optimal EO occurred close to the the value of the baseline. Besides, optimal IO and IC values varies within a wide range (between 49.7 and 100.3, between 39.6 and 96.5), respectively. It was worth noting that overlapping range between 137 and 202 CA becomes longer with the increase of the speed. At the same time, the engine power exhibits a monotonic behavior with the volumetric efficiency. The results represent that the power decreases 2.1% at 17000 rpm and increases at other rotary speeds.

Conclusion

In this paper a numerical approach to increase the volumetric efficiency of a Wankel engine by optimization improvement for port time is presented. The obtained results allow us to draw the following conclusions:

- The computational model used to simulate the working processes in the Wankel engine which adapted peripheral port is able to describe these processes adequately. The predicted results was in accordance with experimental results.
- The optimized results showed that GA was able to find a global optimum in the defined domain.
- The optimal intake open time improves mass-flow rate and flow waves in the engine.
- The angle fluctuation of intake open at TDC is larger than the one of intake close at BDC, when the volumetric efficiency is optimized at constant rotary speed.
- The engine power can be improved by the optimized intake phase.
- The highest volumetric efficiency can be obtained by optimizing the port time, but opening the EO is very late so that a large amount of pumping work is spent resulting in a reduction of the engine thermal efficiency and power.

Acknowledgment

Authors would like to thank National Program on Key Basic Research Project (Grant No. 6132140402) for helping to fund this work.

References

- [1] Picard, M., et al., Predicting Gas Leakage in the Rotary Engine-Part I: Apex and Corner Seals, *ASME*, 138 (2016), 6, ID 062503
- [2] McReynolds, L. A., Small Engines – An Energy Perspective, SAE technical paper, 790477, 1979
- [3] Mahrous, A., et al., A Modeling Study into the Effects of Variable Valve Timing on the Gas Exchange Process and Performance of a 4-Valve di Homogeneous Charge Compression Ignition (HCCI) Engine, *Energy Conversion and Management*, 50 (2009), 2, pp. 393-398
- [4] Nora, M., et al., Effects of Valve Timing, Valve Lift and Exhaust Backpressure on Performance and Gas Exchanging of a Two-Stroke GDI Engine with Overhead Valves, *Energy Conversion and Management*, 123 (2016), Sept., pp. 71-83
- [5] Angelo, A., Experimental Investigation of the Fluid Dynamic Efficiency of a High Performance Multi-valve Internal Combustion engine During the Intake Phase: Influence of Valve-Valve Interference Phenomena, *Thermal Science*, 17 (2013), 1, pp. 25-34
- [6] Niculae, N., et al., Performance Comparison between Hydrogen and Gasoline Fuelled SI Engine, *Thermal Science*, 15 (2011), 4, pp. 1155-1164
- [7] Fontana, G., et al., Effect of Asynchronous Valve Timing on Combustion Characteristic and Performance of a High Speed SI Marine Engine with Five Valves, *Energy Conversion and Management*, 123 (2016), Sept., pp. 185-199
- [8] D'Errico, G., et al., Multi-Objective Optimization of Internal Combustion Engine by Means of 1D Fluid-dynamic Models, *Applied Energy*, 88 (2011), 3, pp. 767-777
- [9] Sher, E., et al., Optimization of Variable Valve Timing for Maximizing Performance of an Unthrottled SI Engine a Theoretical Study, *Energy*, 27 (2002), 8, pp. 757-775
- [10] Zhao, J., et al., Fuel Economy Optimization of an Atkinson Cycle Engine Using Genetic Algorithm, *Applied Energy*, 105 (2013), May, pp. 335-348
- [11] Och, S., et al., Volumetric Efficiency Optimization of a Single-Cylinder DI Diesel Engine Using Differential Evolution Algorithm, *Applied Thermal Engineering*, 108 (2016), Sep., pp. 660-669
- [12] Albrecht, A., et al., 1D Simulation of Turbocharged Gasoline Direct Injection Engine for Transient Strategy Optimization, SAE Technical paper, 2005-01-0693, 2005
- [13] Galindo, J., et al., Solution of the Turbocompressor Boundary Condition for One-Dimensional Gas-Dynamic Code, *Mathematical and Computer Modelling*, 52 (2010), 7-8, pp. 1288-1297
- [14] Wiebe, I., Halbempirische formel durch die verbrennungsgeschwindigkeit, in *Kraftstoffaufbereitung und Verbrennung bei Dieselmotoren*, Spring-Verlag, 1964
- [15] Ma, J., et al., Mathematical Simulation and Study of the Transient Performance of a Rotary Engine, SAE technical paper, 932455, 1993
- [16] Ramos, J., *Internal Combustion Engine Modeling*, Hemisphere Publishing Corporation, New York, USA, 1989
- [17] Guido, A., Predicting the Emissions and Performance Characteristics of a Wankel Engine, SAE technical paper, 740186, 1974
- [18] Zhang, Y., et al., The Study of Turbulent Fluctuation Characteristics in a Small Rotary Engine with a Peripheral Port Based on the Improved Delayed Detached Eddy Simulation Shear-Stress Transport (IDDES-SST) Method, *Energies*, 11 (2018), 3, 642